A Thermodynamic Model of Membrane Humidifiers for PEM Fuel Cell Humidification Control

Dongmei Chen

Huei Peng[1]
e-mail: hpeng@umich.edu

Department of Mechanical Engineering,
University of Michigan, Ann Arbor, MI 48109

Maintaining proper membrane humidity is crucial to ensure optimal operation of a polymer electrolyte membrane fuel cell system. A membrane humidifier using the fuel cell exhaust gas to humidify the dry air is studied in this paper. We first develop a thermodynamic model, which captures the crucial dynamic variables of the humidifier, including the pressure, flow rate, temperature, and relative humidity of the air flow. Steady-state simulations are then conducted to optimize the humidifier design. Subsequently, dynamic simulations are performed to predict the behavior of the humidifier during transient operations typical for automotive applications. A simple proportional controller was designed to control the humidifier operation. [DOI: 10.1115/1.1978910]

1 Introduction

The polymer electrolyte membrane (PEM) fuel cell is considered as one of the most promising alternative automotive power sources to compete with internal combustion (IC) engines due to its lower overall emission and higher efficiency. With the introduction of Honda's first limited-quantity fuel cell vehicle, FCX, in 2002 and a similar offering from Toyota, PEMFC has passed its initial feasibility evaluation stage and is gradually becoming a viable technology to compete with IC engines in the automotive market. To realize its full potential, however, significant improvement is still needed. The improvement includes, but is not limited to, cost and size reduction, improved reliability against fuel variation and impurity, on-board storage, and improved cold-dry environment operability.

One of the key challenges for optimum fuel cell performance is to maintain proper membrane humidity of the PEM fuel cells [1]. Less than full hydration of the membrane will decrease the protonic conductivity and lead to increased resistive loss, decreased net fuel cell stack power [2], and local hot spots that could dramatically reduce the life of the membrane. On the other hand, if excessive water is present in the membrane and/or the gas diffusion layer, a situation commonly known as flooding will occur. Flooding causes the blockage of the gas flow channels, electrodes, and backing layers, and thus bears detrimental effects on the fuel cell performance and life [3,4]. Therefore, it is crucial to control the membrane humidity of the fuel cells to avoid dehydration and flooding. Maintaining proper membrane humidity is especially important in automotive applications where the electric current drawn from the fuel cell changes rapidly with the road load and driver demand. Future automotive fuel cell systems must have desirable membrane humidity under unpredictable power demand and environmental conditions [4,5].

The membrane humidity of PEM fuel cells is characterized by many intrinsic parameters of the membrane, such as the water diffusion coefficient, electro-osmotic drag coefficient, water sorption isotherms, membrane conductivity, and thickness [3,6–9]. These parameters cannot be easily changed after the fuel cell is designed and the membrane is selected. The membrane humidity is also found to be a function of external variables including cell current, the temperature rise inside the fuel cell, and the inlet gas humidity condition [2–4,10,11]. The cell current is determined by the load condition. The temperature rise inside the fuel cell depends on the fuel cell current and is controlled by the cooling system that aims to keep the fuel cell temperature at 80°C. Both of them are hardly controllable during fuel cell operation. However, the inlet gas humidity condition is not affected by the fuel cell operation, and provides the most leverage on controlling the fuel cell membrane humidity. To control the inlet gas humidity condition, a humidifier at the fuel cell inlet can be used. Developing a dynamic model to describe the humidifier transient phenomena is the essential first step before the humidifier control design.

Little information related to the transient humidification phenomena is available in the literature. Even though many theoretical and empirical models have been developed to predict fuel cell membrane humidity, most of them either are for steady-state analysis or are computation intensive. For example, a one-dimensional (1D) steady state PEM fuel cell model was developed to predict the water transport mechanisms and their effects on fuel cell performance [2]. A two-dimensional (2D) steady state PEM fuel cell model was developed to compare the effectiveness of different humidification strategies [1]. A three-dimensional (3D) steady state CFD PEM fuel cell model was developed to predict the temperature distribution inside the fuel cell channels and the effect of heat produced by the fuel cell [10]. Although these models provide useful guidelines for fuel cell design, they usually are only applicable to steady-state operations, and the overall system is optimized accordingly. For automotive applications, the fuel cell has to be controlled to operate at its peak performance under varying load conditions. This calls for dynamic models that are relatively simple and yet accurate enough for control design and analysis.

The purpose of this paper is to develop a control-oriented model that describes the transient thermodynamic behavior of membrane humidifiers. The membrane humidifier outputs are modeled as functions of the time-varying mass flow rates, pressures, humidity, and temperatures of the gases. The model will enable not only steady-state analysis, but also dynamic analysis for transient response and automatic humidification control. The steady-state analysis provides critical insight for the humidifier design optimization. The dynamic analysis is used for developing control algorithms to regulate the vapor concentration of the humidifier outlet gas according to the fuel cell stack operation.

2 Analysis of Membrane Humidification

2.1 Humidification Devices. The reactants entering the fuel cells, if untreated, could have temperature and humidity within a

[1]Corresponding author, Associate Professor, Department of Mechanical Engineering, University of Michigan, Ann Arbor, MI 48109-2133, 734-936-0352.

Contributed by the Dynamic Systems, Measurement, and Control Division of THE AMERICAN SOCIETY OF MECHANICAL ENGINEERS for publication in the ASME JOURNAL OF DYNAMIC SYSTEMS, MEASUREMENT, AND CONTROL. Manuscript received: February 23, 2004; Final revision: October 22, 2004. Associate Editor: Hemant M. Sardar.

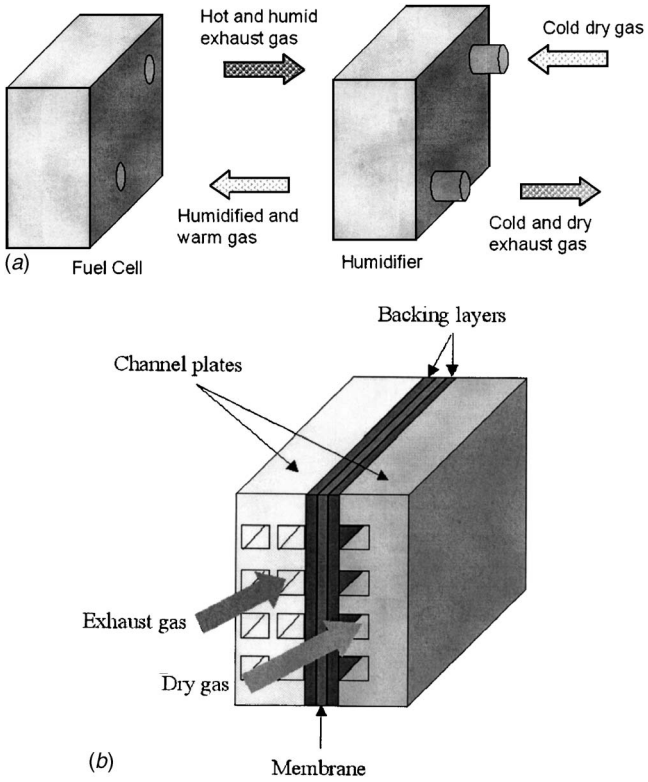

Fig. 1 (*a*) Membrane humidifier integrated with fuel cell stack. (*b*) Humidifier structure.

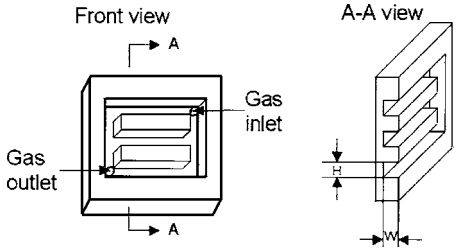

Fig. 2 Humidifier channel plate

wide range and thus significantly affect the performance of PEM fuel cells. To solve this problem, a humidifier at the fuel cell inlet can be used to adjust the inlet reactants relative humidity. Membrane humidity, i.e., membrane water content, varies with the cathode and anode reactants relative humidity. For PEM fuel cell stacks, the goal of a humidifier is to manipulate the reactant relative humidity so that the fuel cell membrane humidity stays close to 100% without flooding.

Other researchers have proposed several PEM fuel cell humidification mechanisms. The most common ones are nozzle spray, gas bubbling, the "enthalpy wheel" [12], and membrane humidification. The nozzle spray and gas bubbling mechanisms do not always provide high relative humidity boost at the operating temperature of PEM fuel cells due to the heat loss of the vaporization process and the low inlet temperature of the reactants. Water heaters can be added to provide additional control authority. However, they are not preferred because of the added weight, complexity, cost, and parasitic loss [13]. The enthalpy wheel device and the membrane humidification mechanism reuse the heat and water vapor exhausted from the fuel cell to heat and humidify the dry gas. They recover some of the fuel cell exhaust energy and help to increase the overall system efficiency. Membrane humidification has been used in several prior studies by other researchers [14–17] and is one of the most promising humidification mechanisms. This paper will focus on membrane humidification as well.

A schematic of the integrated fuel cell and membrane humidifier system is shown in Fig. 1(*a*). The fuel cell exhaust gas is fed to the humidifier to warm up and humidify the dry gas. The humidifier internal structure is described in Fig. 1(*b*). The humidity exchange membrane is sandwiched between the backing layers and flow channel plates. The dry reactant flows into one channel plate and the fuel cell exhaust gas flows into the other one. Water diffuses from one side of the membrane to the other side, while the gases flow in parallel to the hydrated membrane. Nafion[1] membrane is selected as the humidity exchange membrane. The channel plate structure is detailed in Fig. 2. A conventional straight flow channel design is used. The dimensions "H" and "W" in Fig. 2 characterize the channel size. Their effects on the overall humidifier performance will be discussed later.

The flow channel of a humidifier unit is shown in Fig. 3. There are three gas channels in each humidifier unit: A channel "A," which is the humidification channel, a channel "B," which is the heat transfer channel, and a channel "C," which is the exhaust gas channel. The dry inlet gas goes through either channel "A" or channel "B." When the inlet gas passes through channel "A," both heat and water vapor exchanges with channel "C" will occur. On the contrary, when the gas passes through channel "B," only heat exchange will happen. Depending on the position of the sliding plate, the gas will be directed to go through either channel "A" as in Fig. 3(*a*) to be humidified, or channel "B" as in Fig. 3(*b*) to be heated only.

Assuming there are N humidifier units, the number of units designated as type "A" can be any number between 0 and N, depending on the desired relative humidity of the exiting gas. For example, if the desired relative humidity is 100%, the sliding plates are moved so that all the gas goes through "A" channels. Similarly, if the desired relative humidity is 0%, all the "A" channels will be closed. In general, the number of channel "A" will be $0 \leqslant n \leqslant N$, and is calculated based on the fuel cell stack current and the desired relative humidity. It should be noted that the authority of the humidifier in reducing humidity is limited. When the inlet air has a nonzero relative humidity, we will not get 0% at the outlet even though no channel "A" is used.

2.2 Control Volume Definition. To derive the governing thermodynamic equations, we first need to define the control volumes of the humidifier system. For the humidifier design presented in Sec. 2.1, two control volumes are defined as shown in Fig. 4. Control Volume 1 includes either Channel "A" or Channel "B." Control Volume 2 includes Channel "C." For Control Volume 1, the dry gas inlet mass flow rate, pressure, temperature, and relative humidity (RH) are denoted as $M_{1,\text{in}}$, $P_{1,\text{in}}$, $T_{1,\text{in}}$, and $\Phi_{1,\text{in}}$, respectively. The gas outlet mass flow rate, pressure, temperature, and RH are denoted as $M_{1,\text{out}}$, $P_{1,\text{out}}$, $T_{1,\text{out}}$, and $\Phi_{1,\text{out}}$, respectively. If Control Volume 1 includes Channel "A," both vapor transfer $M_{1,v,\text{tr}}$ and heat transfer $\mathcal{Q}_1$ occur. If Control Volume 1 includes Channel "B," only heat transfer $\mathcal{Q}_1$ occurs. For Control Volume 2, the exhaust gas inlet (exhausted from fuel cell) mass flow rate, pressure, temperature, and RH are denoted as $M_{2,\text{in}}$, $P_{2,\text{in}}$, $T_{2,\text{in}}$, and $\Phi_{2,\text{in}}$, respectively. The exhaust gas outlet mass flow rate, pressure, temperature, and RH are denoted as $M_{2,\text{out}}$, $P_{2,\text{out}}$, $T_{2,\text{out}}$, and $\Phi_{2,\text{out}}$, respectively. The dry gas and the exhaust gas can flow in several patterns (parallel, cross, and counter flow patterns). Figure 4 shows that the dry gas and the exhaust gas flow in the counter flow arrangement.

[1]Nafion is a trademark of DuPont Company

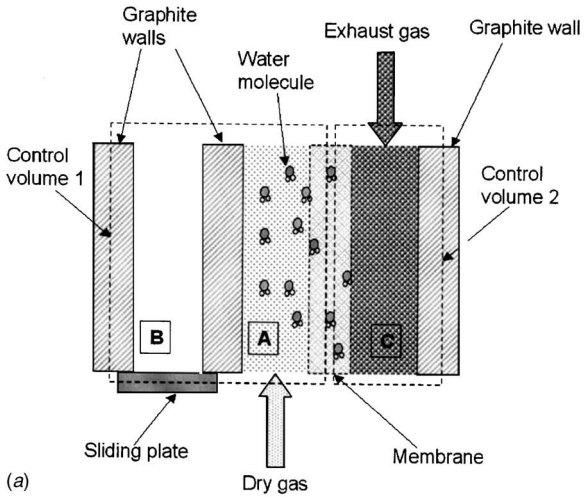

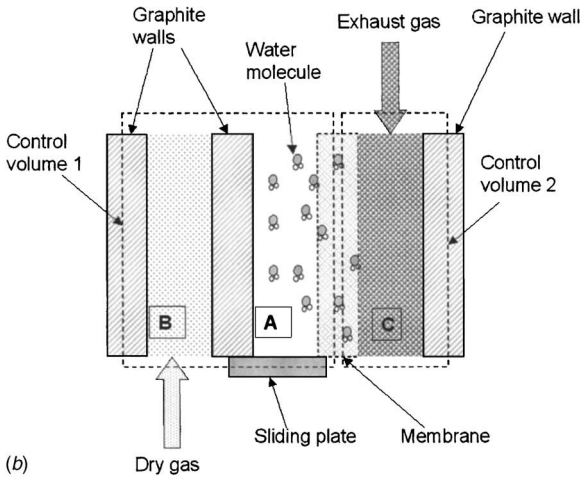

Fig. 3 (*a*) Three channels of a humidifier unit: Exhaust gas channel (right), humidification channel (center, open), and heat exchanging channel (left, closed). (*b*) Three channels of a humidifier unit: Exhaust gas channel (right), humidification channel (center, closed), and heat exchanging channel (left, open).

3 Thermodynamic Modeling of Membrane Humidifier

3.1 Assumptions. The model assumptions are:

- The flows in both control volumes are fully developed laminar flows.
- All gases follow the ideal gas law.
- The humidifier units are well insulated from its surroundings thus heat transfer occurs only across the membrane, between channel "A" and "C" or "B" and "C" (which are assumed to have the same heat conductivity).
- The kinetic and potential energies of the gas molecules are neglected.
- No external work is done to the system.
- The flow specific heats are constant.
- The overall convection heat transfer coefficient is constant.
- The membrane water transfer is a function of water concentration and temperature gradients.
- The nominal fuel cell exhaust gas temperature is assumed to be 80°C.
- The following inlet gas properties are the inputs to the dynamic system: $M_{1,\text{in}}$, $P_{1,\text{in}}$, $T_{1,\text{in}}$, $\Phi_{1,\text{in}}$, $M_{2,\text{in}}$, $P_{2,\text{in}}$, $T_{2,\text{in}}$, and $\Phi_{2,\text{in}}$.

3.2 Dynamic Equations. The governing equations are derived to describe the transient behavior of the gases in the two control volumes based on thermodynamics principle, mass continuity equations, heat transfer theories, and experimental results (published in the literature)for membrane diffusion.

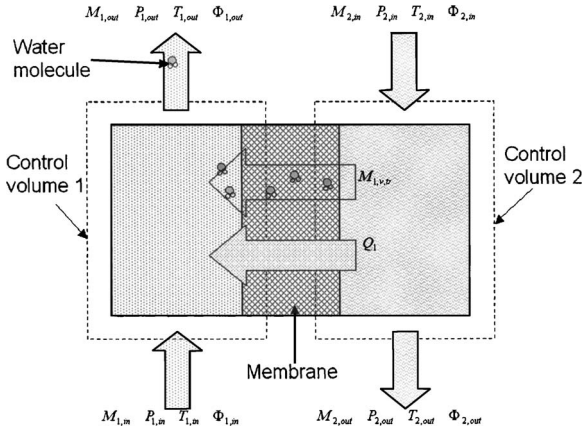

Fig. 4 Control volumes of one humidifier unit

3.2.1 The First Law of Thermodynamics. Based on the first law of thermodynamics, the governing equation for control volumes 1 and 2 is [18]:

$$\sum \frac{dm_{k1,k2,\text{out}}}{dt} h_{k1,k2,\text{out}} = \frac{dQ_{k1}}{dt} + \sum \frac{dm_{k1,k2,\text{in}}}{dt} h_{k1,k2,\text{in}} + \frac{n}{N}\frac{dm_{k1,v,\text{tr}}}{dt} h_{\text{tr}} - \left[\frac{dm_{k1,k2}}{dt} u_{k1,k2} + \frac{du_{k1,k2}}{dt} m_{k1,k2} \right] \quad (1)$$

where $m_{k1,k2,\text{in}}$ is the mass entering in the control volume, $m_{k1,k2,\text{out}}$ is the mass leaving the control volume, and $m_{k1,v,\text{tr}}$ is the mass transferred across the membrane. The third term on the right hand side of the equation shows the effect of control, where n denotes the number of units using channel "A," and N is the total number of humidifier units. The equations governing the gas enthalpy h and internal energy u are

$$\frac{du_{k1,k2}}{dt} = Cv_{k2}\frac{dT_{k1}}{dt} \quad (2)$$

$$\frac{dh_{k1,k2,k3}}{dt} = Cp_{k2}\frac{dT_{k1,k3}}{dt} \quad (3)$$

where the subscripts $k1$, $k2$, and $k3$ are explained in Table 1. Since the humidifier is isolated from its surroundings, dQ_1/dt is equal to $-dQ_2/dt$. In addition, because of mass continuity, $dm_{1,v,\text{tr}}/dt$ is equal to $-dm_{2,v,\text{tr}}/dt$.

3.2.2 Vapor Mass Diffusion. Vapor mass transfer $\dot{m}_{k1,v,\text{tr}}$ occurs between the two control volumes when channel "A" is used, due to the humidity gradient across the membrane. The amount of vapor mass transferred would be determined by the membrane coefficient of diffusion and the gradient of RH across the membrane, and can be written as [1,4]

$$\frac{dm_{k1,v,\text{tr}}}{dt} = D_w \frac{C_2 - C_1}{t_m} M_v A \quad (4)$$

where M_v is the vapor molar mass, C_1 and C_2 represent water concentrations in Control Volumes 1 and 2, respectively, and will be explained in Eq. (7). The membrane coefficient of diffusion, D_w is determined by the following empirical equation [2,4]

Table 1 Subscripts parameter table

k_1	k_2	k_3
1 (Control Volume 1)	g (dry gas) or v (vapor) in Control Volume 1	In, out, or tr (inlet, outlet, or transfer)
2 (Control Volume 2)	Ex (exhaust gas) or v (vapor) in Control Volume 2	In, out, or tr (inlet, outlet, or transfer)

$$D_w = D_\lambda e^{2416(1/303 - 1/T_m)} \tag{5}$$

where T_m is the membrane temperature. The coefficient D_λ is determined empirically [2,4] and has a piecewise-linear form:

$$D_\lambda = \begin{cases} 10^{-6} & \lambda_m < 2 \\ 10^{-6}(1 + 2(\lambda_m - 2)) & 2 \leqslant \lambda_m \leqslant 3 \\ 10^{-6}(3 - 1.67(\lambda_m - 3)) & 3 < \lambda_m < 4.5 \\ 1.25^{*}10^{-6} & \lambda_m \geqslant 4.5 \end{cases} \tag{6}$$

where λ_m is the membrane water content which will be defined in Eq. (8). The water concentration of both Channel "A" and Channel "C" is

$$C_{k1} = \frac{\rho_{m,\mathrm{dry}}}{M_{m,\mathrm{dry}}} \lambda_{k1} \tag{7}$$

where $\rho_{m,\mathrm{dry}}$ is the membrane dry density, $M_{m,\mathrm{dry}}$ is the membrane dry equivalent weight. λ_{k1} is the water content of Control Volumes 1 or 2. Both λ_m and λ_{k1} can be expressed as

$$\lambda_{k4} = (0.043 + 17.81 a_{k4} - 39.85 a_{k4}^2 + 36.0 a_{k4}^3) \tag{8}$$

where $k4$ can be 1, 2 (the two control volumes) or m (for the membrane). For both control volumes, the water activity is defined as

$$a_{k1} = \frac{P_{k1,v}}{P_{k1,\mathrm{sat}}} \tag{9}$$

where $P_{k1,v}$ is the partial pressure of the vapor stored in Control Volume $k1$, and is assumed to be equal to $P_{k1,v,\mathrm{out}}$. $P_{k1,\mathrm{sat}}$ is the saturation pressure of the vapor stored in Control Volume $k1$, which is determined by [19]

$$\log_{10}(P_{k1,\mathrm{sat}}) = -1.69 \cdot 10^{-10} T_{k1}^4 + 3.85 \cdot 10^{-7} T_{k1}^3 - 3.39 \cdot 10^{-4} T_{k1}^2 + 0.143 T_{k1} - 20.92 \tag{10}$$

where $T_{k1} = T_{k1,\mathrm{out}}$ due to the uniformity assumption. The membrane water activity and temperature are calculated from

$$a_m = \frac{a_1 + a_2}{2} \tag{11}$$

and

$$T_m = \frac{T_1 + T_2}{2} = \frac{T_{1,\mathrm{in}} + T_{1,\mathrm{out}} + T_{2,\mathrm{in}} + T_{2,\mathrm{out}}}{4} \tag{12}$$

3.2.3 Heat Transfer. The heat transfer rate between the two control volumes is [20]

$$\frac{dQ_1}{dt} = UA\Delta T_{2/1} \tag{13}$$

where A is the membrane area, $\Delta T_{2/1}$ is the log mean temperature difference between the two control volumes, and U is the overall heat transfer coefficient defined as [20]

$$U = \frac{\bar{h}}{2} \quad \bar{h} = \frac{kN_{uD}}{D_h} \tag{14}$$

where k is the membrane thermal conductivity, N_{uD} is the Nusselt number, and D_h is the channel hydraulic diameter. For parallel flow arrangement, the log mean temperature difference is calculated from

$$\Delta T_{2/1} = \frac{(T_{2,\mathrm{in}} - T_{1,\mathrm{in}}) - (T_{2,\mathrm{out}} - T_{1,\mathrm{out}})}{\ln((T_{2,\mathrm{in}} - T_{1,\mathrm{in}})/(T_{2,\mathrm{out}} - T_{1,\mathrm{out}}))} \tag{15a}$$

For counter flow arrangement, the log mean temperature difference is calculated from

$$\Delta T_{2/1} = \frac{(T_{2,\mathrm{in}} - T_{1,\mathrm{out}}) - (T_{2,\mathrm{out}} - T_{1,\mathrm{in}})}{\ln((T_{2,\mathrm{in}} - T_{1,\mathrm{out}})/(T_{2,\mathrm{out}} - T_{1,\mathrm{in}}))} \tag{15b}$$

3.2.4 Ideal Gas Law. Applying the ideal gas law to the two control volumes, the following equations are obtained

$$P_{k1,k2,\mathrm{out}} V_{k1} = R_{k2} T_{k1,\mathrm{out}} m_{k1,k2} \tag{16}$$

$$\omega_{1,k3} = \frac{M_v P_{1,v,k3}}{M_g P_{1,g,k3}} \tag{17a}$$

$$\omega_{2,k3} = \frac{M_v P_{2,v,k3}}{M_{\mathrm{ex}} P_{2,\mathrm{ex},k3}} \tag{17b}$$

$$\Phi_{k1,k3} = \frac{P_{k1,v,k3}}{P_{k1,\mathrm{sat},k3}} \tag{18}$$

where V_{k1} is the volume of the control volume $k1$, R_{k2} is the gas constant, M_v, M_g, and M_{ex} are the molar mass of vapor, dry gas, and exhaust gas, respectively. Then the outlet mass flow rates are obtained from

$$\frac{dm_{1,g,k3}}{dt} = \frac{1}{1 + \omega_{1,k3}} \frac{dm_{1,k3}}{dt} \tag{19a}$$

$$\frac{dm_{2,\mathrm{ex},k3}}{dt} = \frac{1}{1 + \omega_{2,k3}} \frac{dm_{2,k3}}{dt} \tag{19b}$$

3.2.5 Conservation of Mass. The mass conservation equations for the two control volumes are

$$\frac{dm_{k1,k2}}{dt} = \sum \frac{m_{k1,k2,\mathrm{in}}}{dt} - \sum \frac{m_{k1,k2,\mathrm{out}}}{dt} \tag{20}$$

which can be used to calculate the gas or water vapor mass stored in Control Volumes, $m_{k1,k2}$.

3.2.6 Flow Restriction Equation. The gas mass flow rates of the two control volumes are constrained by the intake areas and can be approximated by the orifice equation [21]

$$\frac{dm_{k1,\mathrm{out}}}{dt} = Cr_{k1} \sqrt{P_{k1,\mathrm{out}} - P_{k1,\mathrm{sub}}} \tag{21}$$

where Cr_{k1} is the orifice restriction constant which is a function of the orifice size and the gas density and can be obtained through either theoretical calculation [21] or testing. $P_{k1,\mathrm{sub}}$ is the pressure at the subsequent system. For example, if the outlet is connected to the atmosphere, then $P_{k1,\mathrm{sub}}$ is the atmosphere pressure.

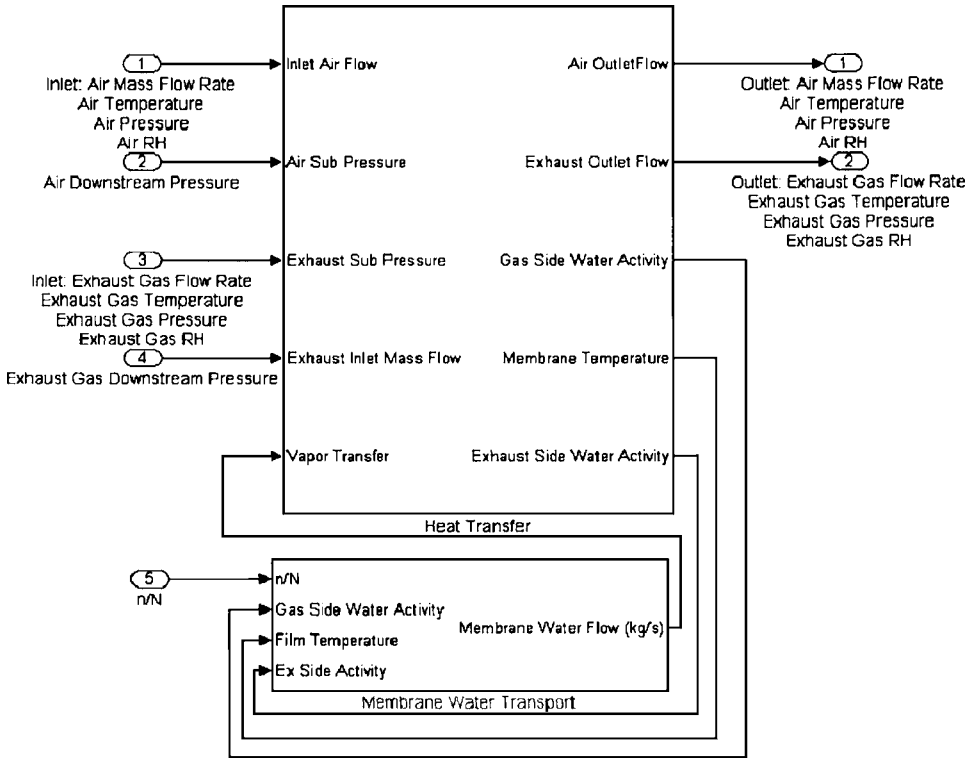

Fig. 5 Humidifier model in SIMULINK

4 Simulations

A mathematic model is developed in the SIMULINK environment based on Eqs. (1)–(21) presented above. The model is nonlinear and its input-output and state variables are summarized as follows. The six state variables are $x=[m_{1,g}\ m_{1,v}\ T_{1,\text{out}}\ m_{2,\text{ex}}\ m_{2,v}\ T_{2,\text{out}}]^T$, the control input is $u=1/N[n]$, and the uncontrolled inputs (disturbance inputs) are $w=[\dot{m}_{1,\text{in}}\ T_{1,\text{in}}\ P_{1,\text{in}}\ \Phi_{1,\text{in}}\ \dot{m}_{2,\text{in}}\ T_{2,\text{in}}\ P_{2,\text{in}}\ \Phi_{2,\text{in}}]^T$. The performance variable, which characterizes the humidifier operation, is $z=[\dot{m}_{1,v,\text{tr}}]=f(m_{1,g}\ m_{1,v}\ T_{1,\text{out}}\ m_{2,\text{ex}}\ m_{2,v}\ T_{2,\text{out}})$. Possible measurements include $y=[\dot{Q}_1\ \dot{m}_{1,v,\text{tr}}\ \dot{m}_{1,\text{out}}\ \dot{m}_{2,\text{out}}\ \Phi_{1,\text{out}}\ \Phi_{2,\text{out}}\ P_{1,\text{out}}\ P_{2,\text{out}}]^T$, all or part of the measurements can be used in the control signal calculation.

The Simulink diagram of the model is shown in Fig. 5, and its heat transfer sub-model is highlighted in Fig. 6. The arrows going into the left side of the system are system inputs, and the arrows going out of the right side of the system are system outputs. The model was developed for an imagined cathode humidifier used for a 75 kW fuel cell stack designed for the Ford P2000 concept electrical vehicle. An earlier analysis shows that adding an anode humidifier bears little benefit [22]. Therefore, we focus on the effects of a cathode humidifier in this paper. A simulation model for this P2000 fuel cell stack has been described in an earlier publication [4]. By combining the developed humidifier model and the fuel cell stack model developed in [4], an in-depth analysis of the overall system becomes possible. The parameters of the humidifier system are listed in Table 2.

When a fuel cell stack operates at different power levels, the amount of water generated will be proportional to the stack current. Therefore, the amount of vapor to be added to its inlet reactants change accordingly. In particular, the amount of water vapor needed at the humidifier varies with the stack current and environment air temperature and humidity. Assuming the inlet air is at 0% RH and 80°C, to maintain 100% membrane RH, the required vapor transfer rate added to the cathode inlet reactants is shown in Fig. 7. By adding vapor at this rate, we will achieve the highest RH without flooding the channels. For the fuel cell stack studied, the maximum additional vapor needed at the humidifier is 0.0042281 kg/s at the current level of 90 A. Starting from the low current, the water added is essentially proportional to stack current. When the stack current becomes higher than 90 A, more water will be generated at the cathode and thus the amount of water needed decreases. When the current is higher than 250 A, the fuel cell stack is over saturated even with 0% inlet air RH. To avoid flooding the fuel cell stack, water needs to be removed (which, of course, is beyond the ability of our humidifier system). The negative number shown in Fig. 7 means the water needs to be removed from the stack.

5 Results and Discussion

5.1 Steady State Results. Several simulations were conducted under steady-state conditions to illustrate the characteristics of the integrated system as well as to show how the model can be used for humidifier design optimization. The performance goal is to achieve the desired humidifier vapor transfer rate that keeps the optimal air RH at the fuel cell cathode inlet without flooding the fuel cell stack at its operating temperature of 80°C. Once the stack current is given, the required vapor transfer rate can be calculated, as depicted in Fig. 7. We first study the effect of flow channel arrangement on system performance. The analysis results of counter flow versus parallel flow arrangements, under the condition that 100% air go through Channel "A," are shown in Fig. 8. The x axis is the fuel cell inlet air flow rate, the starting and the ending points correspond to the stack currents of 60 and 310 A, respectively. The first and the second plots in Fig. 8 show that the counter flow arrangement is more effective in heat transfer. The third plot shows that the counter-flow arrangement also allows more water vapor to pass through the membrane. Therefore, the counter flow arrangement is selected over its parallel flow counterpart.

The channel cross-section design of the humidifier units is another important factor affecting the system performance. Keeping

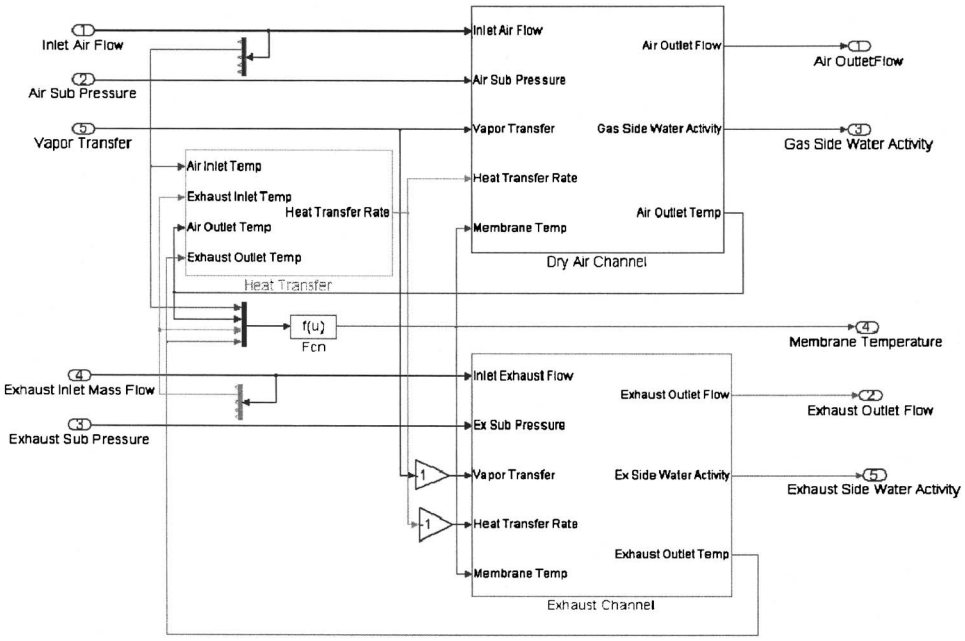

Fig. 6 Heat transfer sub-model in SIMULINK

the unit number the same, three channel cross section areas are compared. The cross section size is determined by the channel width W and height H as shown in Fig. 2. We selected the number of humidifier cells to be 381 for the optimization study, the same as the number of cells of the P2000 stack. The result of keeping W at 1 mm and the number of units at 381 is shown in Fig. 9. It can be seen that 1 mm $\times$ 4 mm channels provide the highest air outlet temperature and vapor transfer rate. This is because that 4 mm, which is along the membrane surface, allows more surface area to conduct heat and mass transfer than the 2 and 1 mm cases. However, the membrane selected for the humidifier is very thin, only 0.0025 cm thick. A 4 mm gap between the supporting walls might cause the membrane to deform excessively if there is pressure gradient across the membrane. A careful flow channel simulation and structure integrity study is required if the 1 mm $\times$ 4 mm case is to be used.

The results with fixed H at 1 mm and changing W between 0.5 and 1 mm are shown in Fig. 10. Plot 1 of Fig. 10 shows that under the same input condition, the configuration 0.5 mm $\times$ 1 mm with 381 units has higher outlet air temperature than 1 mm $\times$ 1 mm with 381 does. Plot 2 shows that under the same input condition, both configurations generate similar vapor transfer rates. This is because both of them have the same membrane area. The vapor transfer rate across the membrane is mainly a function of the membrane temperature and RH gradient, which are similar for these two cases in this simulation.

Another observation is that the air outlet temperature is lower than the fuel cell operation temperature for the simulated inlet temperature of 30°C and fuel cell exhaust gas temperature of 80°C. If the fuel cell operation requires 100% RH at the air inlet, a heater is required to heat the air before it enters the humidifier. Otherwise, the air with 100% RH at low temperature will not have 100% RH once it is heated to the fuel cell temperature.

The number of humidifier units is also an important design factor for humidifier sizing. Keeping all the other parameters fixed and assuming all the air goes through Channel "A," four different unit numbers are simulated and the result is shown in Fig. 11. It can be seen that the outlet air temperature and vapor transfer rate

Table 2 Humidifier parameters for P2000 75 kW fuel cell stack

Membrane cross section area	280 cm^2
Membrane thickness	0.0025 cm
Membrane dry density	0.001 kg/cm^3
Membrane dry equivalent weight	1.0 kg/mol
Number of humidifier unit	571
Dimension "H"	0.001 m
Dimension "W"	0.001 m
Channel hydraulic diameter	0.001 m
Nusselt number	5.4
Humidifier air channel "A" volume	0.015 m^3
Humidifier air channel "B" volume	0.015 m^3
Humidifier exhaust channel "C" volume	0.015 m^3
Heat transfer efficiency	80%
Air thermal conductivity	0.028 W/m·K
Air channel orifice restriction coefficient	0.42
Exhaust gas channel orifice restriction coefficient	0.42

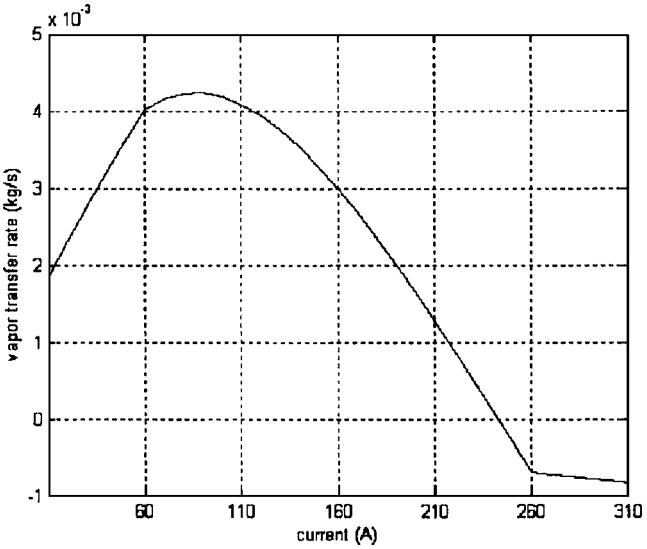

Fig. 7 Required vapor rate added to the P2000 cathode inlet at 80°C

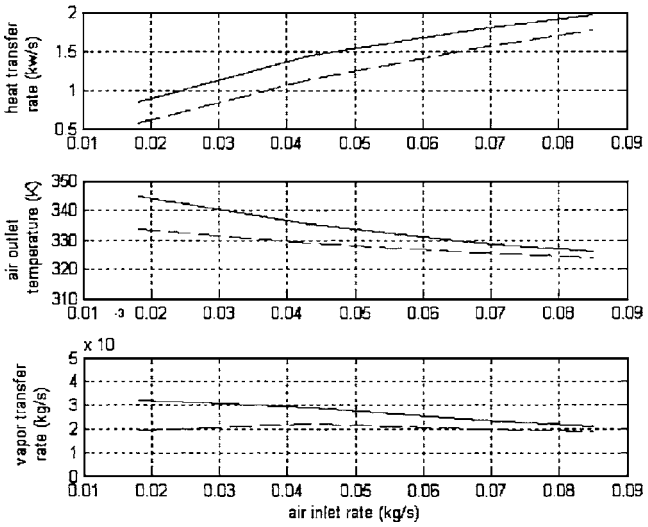

Fig. 8 Counter flow vs parallel flow arrangements. Solid line: Counter flow; Dashed line: Parallel flow.

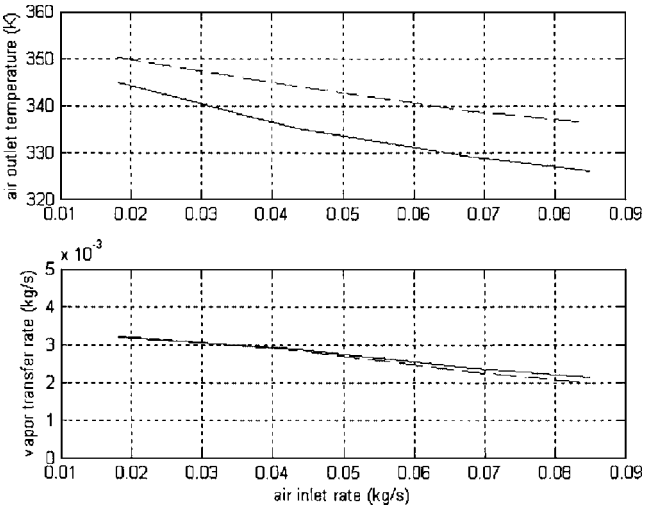

Fig. 10 Comparison of two different cross-section designs with constant 381 units with varying channel width "*W*". Solid line: 1 mm×1 mm; Dashed line: 0.5 mm×1 mm.

increase with the number of humidifier units increasing. Figure 7 shows that the worst-case requires vapor transfer rate of 0.004 2281 kg/s at about 90 A. The dotted line in plot 2 of Fig. 11 meets this requirement. For 1 mm×1 mm cross-section configuration, 571 units with properly controlled n/N can generate the vapor transfer rate shown in Fig. 7.

5.2 Dynamic Results. When the humidifier is used in automotive applications, the operating conditions (power, air flow, etc.) are constantly changing. A simulation with two-step changes in airflow is shown in Fig. 12.

Figure 12 shows that the humidifier system response has large transient dynamics after each step input. The transient errors may affect the fuel cells performance in two ways. First, the initial outputs may affect the vehicle drivability—the passengers may feel the torque disruption due to the transient effect. A quantified systematic study on the integrated humidifier and the fuel cell stack in a vehicle will provide a quantified measure on this effect. Secondly, the transient response may adversely affect the fuel cell life, e.g., due to flooding or dehydration. Adding low pass filter to the fuel cell stack power demand, and augment it with an energy storage element (e.g., battery or ultra-capacitor) may solve the drivability problem. However, this may not be enough to prevent flooding or dehydration. In this case, a properly designed active controller is necessary to reduce the transient error. For instance, the second plot of Fig. 12 shows that if the humidifier is not actively controlled, the membrane vapor transfer rate has undershoot that results in inadequate water vapor is added to the system. When a simple P controller is added to control the number of humidifying units "n," the transient effect will reduce. The control block diagram is shown in Fig. 13. The P control law uses a proportional gain of 1800, and rounded down to obtain the final control "n." The simulation results is shown in Fig. 14, which reveals that the simple P controller increases the amount of water added to the system from the solid line to the dashed line so that the undershoot is decreased and more water vapor is added to the system. More control study will be conducted to search for the optimum control law that results in minimum or zero undershoot.

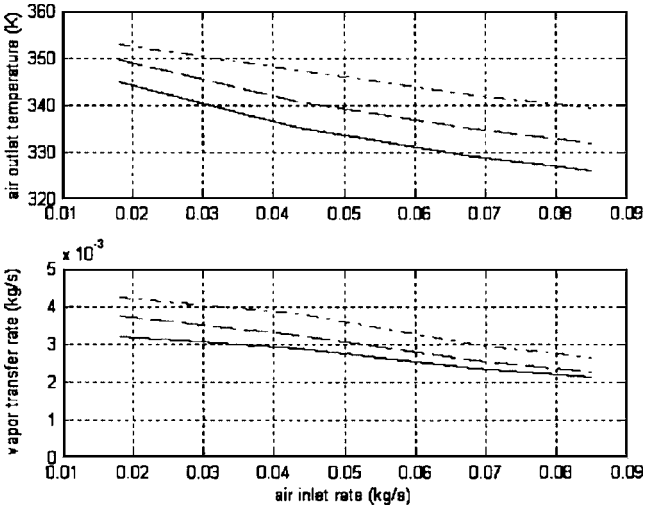

Fig. 9 Comparison of three different cross-section designs with constant 381 units with varying channel height "H". Solid line: 1 mm×1 mm; Dashed line: 1 mm×2 mm; Dash-dot line: 1 mm×4 mm.

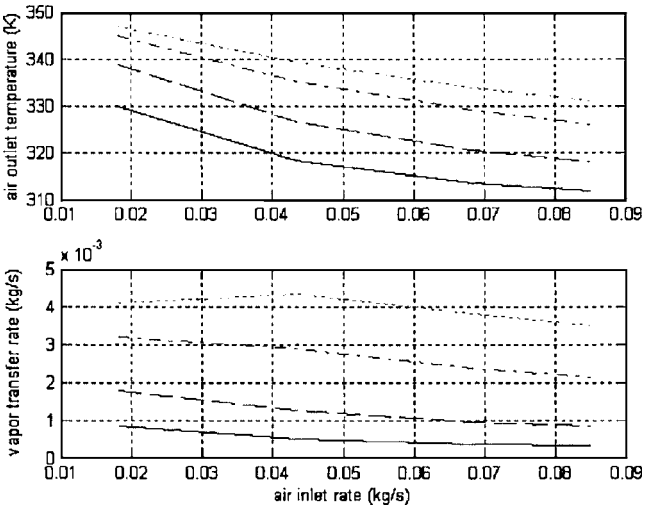

Fig. 11 Comparison of four different unit numbers with 1 mm×1 mm channel cross section. Solid line: 95 units; Dashed line: 190 units; Dash-dot line: 381 units; Dotted line: 571 units.

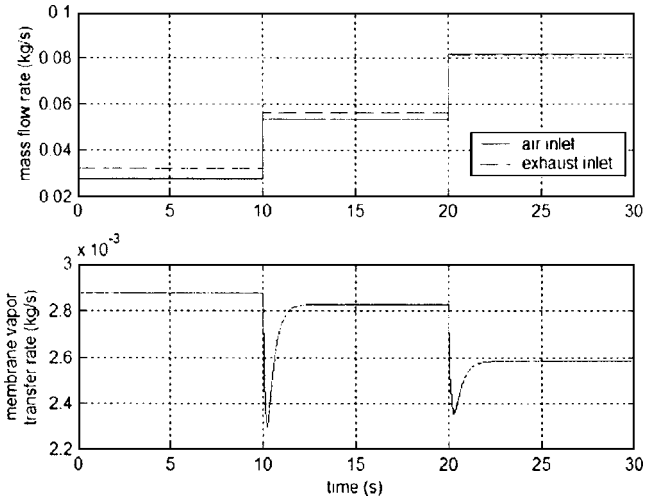

Fig. 12 Dynamic response of the membrane vapor transfer rate under step inputs

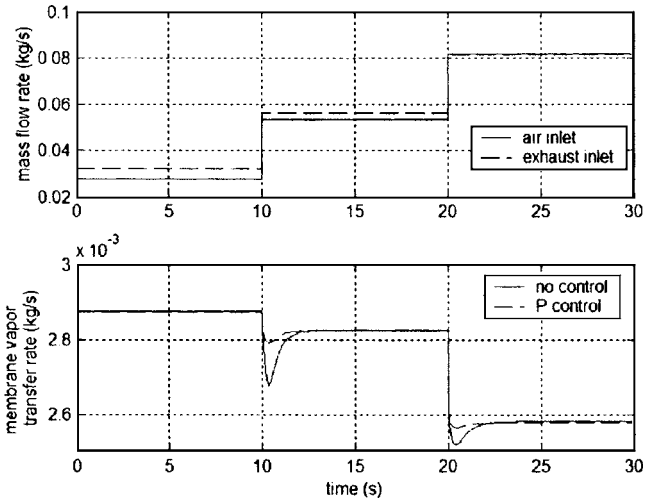

Fig. 14 Membrane vapor transfer rate under two conditions: No control vs *P* control

6 Conclusions

A thermodynamic model was developed for a membrane humidifier of a PEM fuel cell system, which allows dry inlet air to be humidified by the fuel cell exhaust gas. This model includes crucial dynamic variables of the humidifier such as the airflow pressure, flow rate, temperature, and relative humidity. This model enables both steady state analysis for design optimization and dynamic analysis for transient response and active control. Simulations were performed to identify the minimum number of units necessary for a target fuel cell stack. The channel flow structures, dimensions, and cross-section geometry are also studied. The humidifier transient phenomena were captured and a simple *P* control strategy was employed to reduce the transient effect over the system performance. The integration of the humidifier and the fuel cell, and the impact of the humidifier on the fuel cell performance will be studied in the future.

Acknowledgments

The authors wish to acknowledge the support from the University of Michigan Rackham Graduate School Fellowship, and the valuable inputs from Jay T. Pukrushpan, Chan-Chiao Lin, Sangseok Yu, and Professor Claus Borgnakke.

Nomenclature

A = Humidifier membrane area (cm^2)
a = Water activity
C = Water concentration (mol/cm^3)
Cp = Specific heat of constant pressure ($J \cdot kg^{-1} \cdot K^{-1}$)
Cr = Orifice restriction constant
Cv = Specific heat of constant volume ($J \cdot kg^{-1} \cdot K^{-1}$)
D_h = Channel hydraulic diameter (m)
D_w = Membrane diffusion coefficient (cm^2/s)
h = Enthalpy (J)
$\bar{h}$ = Heat transfer coefficient ($W/m^2 \cdot K$)
k = Membrane thermal conductivity (W/m·K)
m = Mass (kg)
M = Molecular mass (kg/mol)
$M_{m,\mathrm{dry}}$ = Membrane dry equivalent weight (kg/mol)
N = Total numbers of humidifier units
n = No. of humidifier units with "A" opened
N_{uD} = Nusselt number
P = Pressure (Pa)
R = Gas constant ($J \cdot kg^{-1} \cdot K^{-1}$)
T = Temperature (K)
t = Time (s)
t_m = Membrane thickness (cm)
Q = Heat (J)
u = Internal energy (J) or system input
U = Overall heat transfer coefficient ($W/m^2 \cdot K$)
V = Volume (m^3)
x = System state vector
y = System measurements
ϕ = Relative humidity
λ = Water content
ρ = Density (kg/cm^3)
ω = Humidity ratio

Subscripts

1 = Control volume 1
2 = Control volume 2
a = Air
ex = Exhaust gas
g = Dry gas
in = Inlet
m = Membrane
out = Outlet
sat = Saturation
v = Vapor

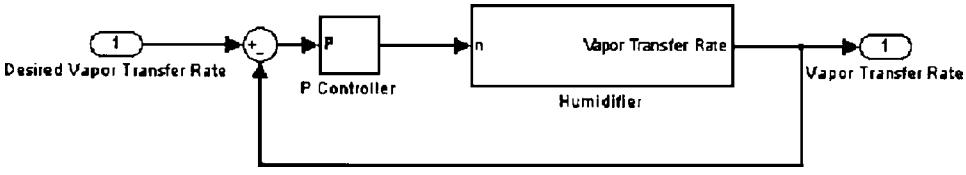

Fig. 13 Humidifier control block diagram

References

[1] T. V. Nguyen and R. E. White, 1993, "A Water and Heat Management Model for Proton-Exchange-Membrane Fuel Cells," J. Electrochem. Soc., **140**, No. 8, pp. 2178–2186.

[2] T. E. Springer, T. A. Zawodzinski, and S. Gottesfeld, 1991, "Polymer Electrolyte Fuel Cell Model," J. Electrochem. Soc., **138**, No. 8, pp. 2334–2342.

[3] M. Ceraolo, C. Miulli, and A. Pozio, 2003, "Modelling Static and Dynamic Behavior of Proton Exchange Membrane Fuel Cells on the Basis of Electrochemical Description," J. Power Sources, **113**, pp. 131–144.

[4] J. T. Pukrushpan, H. Peng, and A. G. Stefanopoulou, "Simulation and Analysis of Transient Fuel Cell System Performance Based on a Dynamic Reactant Flow Model," Proceeding of 2002 ASME International Mechanical Engineering Congress & Exposition, New Orleans, Louisiana.

[5] P. Sridhar, R. Perumal, N. Rajalakshmi, M. Raja, and K. S. Dhathathreyan, 2001, "Humidification Studies on Polymer Electrolyte Membrane Fuel Cell," J. Power Sources, **101**, pp. 72–78.

[6] K. Broka and P. Ekdunge, 1997, *Oxygen and Hydrogen Permeation Properties and Water Uptake of Nafion 117 Membrane and Recast Film for PEM Fuel Cell*, Sweden, Chapman & Hall.

[7] G. J. M. Janssen and M. L. J. Overvelde, 2001, "Water Transport in the Proton-Exchange-Membrane Fuel Cell: Measurements of the Effective Drag Coefficient," J. Power Sources, **101**, pp. 117–125.

[8] C. S. Fadley and R. A. Wallace, "Electopolymer Studies-II. Electrical Conductivity of a Polystyrene Sulfonic Acid Membrane," Journal of Electrochemical Society, Solid State Science, December, 1968.

[9] D. R. Morris and X. Sun, 1993, "Water-Sorption and Transport Properties of Nafion 117H," J. Appl. Polym. Sci., **50**, pp. 1445–1452.

[10] S. Shimpalee and S. Dutta, 2000, "Numerical Prediction of Temperature Distribution in PEM Fuel Cells," Journal of Numer. Heat Transfer, Part A: Applications, **38**, pp. 111–128.

[11] S. Ahmed, J. Kopasz, R. Kumar, and M. Krumpelt, 2002, "Water Balance in a Polymer Electrolyte Fuel Cell System," J. Power Sources, **112**, pp. 519–530.

[12] R. A. Dubose, *Enthalpy Wheel Humidifiers*, Presentation from 2002 Fuel Cell Seminar.

[13] D. Chu and R. Z. Jiang, 1999, "Performance of Polymer Electrolyte Membrane Fuel Cell (PEMFC) Stacks, Part I. Evaluation and Simulation of an Air-Breathing PEMFC Stack," J. Power Sources, **83**, pp. 128–133.

[14] K. H. Choi, D. J. Park, Y. W. Rho, Y. T. Kho, and T. H. Lee, 1998, "A Study of the Internal Humidification of An Integrated PEMFC Stack," J. Power Sources, **74**, pp. 146–150.

[15] S. Miachon and P. Aldebert, 1995, "Internal Hydration H2/O2 100 cm2 Polymer Electrolyte Membrane Fuel Cell," J. Power Sources, **56**, pp. 31–36.

[16] D. Staschewski and Z. Q. Mao, 1999, "Hydrogen-Air PEMFC Operation with Extraordinarily Low Gas Pressures and Internal Humidification-Conception and Experimental Prototype Stack," Int. J. Hydrogen Energy, **24**, pp. 543–548.

[17] F. N. Buchi and S. Srinivasan, 1997, "Operating Proton Exchange Membrane Fuel Cells without External Humidification of the Reactant Gases-Fundamental Aspects," J. Electrochem. Soc., **144**, No. 8, pp. 2767–2772.

[18] R. E. Sonntag, C. Borgnakke, and G. J. Van Wylen, 1998, *Fundamentals of Thermodynamics*, 5th ed., Wiley, New York.

[19] J. T. Pukrushpan, "Modeling and Control of PEM Fuel Cell Systems and Fuel Processors," Ph.D. Dissertation, University of Michigan, 2003.

[20] F. P. Incropera and D. P. DeWitt, 1996, *Introduction to Heat Transfer*, 3rd ed., Wiley, New York.

[21] D. F. Young, *A Brief Introduction to Fluid Mechanics*, 2nd ed., Wiley, New York, 2001.

[22] D. Chen and H. Peng, "Modeling and Simulation of a PEM Fuel Cell Humidification System," Proceeding of 2004 American Control Conference, Boston, Massachusetts.